Coherent optical control of the wave function of zero dimensional exciton polaritons

R. Cerna[1*], D. Sarchi[2†], T. K. Paraïso[1], G. Nardin[1], Y. Léger[1], M. Richard[1‡], B. Pietka[1], O. El Daif[1§], F. Morier-Genoud[1], V. Savona[2], M. T. Portella-Oberli[1], B. Deveaud-Plédran[1]
[1] *Institut de Photonique et d'Électronique Quantiques, École Polytechnique Fédérale de Lausanne (EPFL), CH-1015 Lausanne*
[2] *Institute of Theoretical Physics, Ecole Polytechnique Fédérale de Lausanne EPFL, CH-1015 Lausanne, Switzerland*
(Dated: September 2, 2009)

Control of the wave function of confined microcavity polaritons is demonstrated experimentally and theoretically by means of tailored resonant optical excitation. Three dimensional confinement is achieved by etching mesas on top of the microcavity spacer layer. Resonant excitation with a continuous wave laser locks the phase of the discrete polariton states to the phase of the laser. By tuning the energy and momentum of the laser, we achieve precise control of the momentum pattern of the polariton wave function. This is an efficient and direct way for quantum control of electronic excitations in a solid.

PACS numbers: 71.36.+c, 71.35.-y, 78.55.Cr

Polaritons in semiconductor microcavities are hybrid quasiparticles consisting of a superposition of photons and excitons. Due to their photon component, polaritons are characterized by a quantum coherence length in the several micron range. Owing to their exciton content, they display sizeable interactions, both mutual and with other electronic degrees of freedom. These unique features have produced striking matter wave phenomena, such as Bose-Einstein condensation[1, 2], or parametric processes [3, 4] able to generate entangled polariton states [5, 6].

The key feature of polaritons with respect to confinement is their very small effective mass, which is about 10^5 times smaller than the free electron mass. Hence, confinement within micrometer sized traps is sufficient to produce an atom-like spectrum with discrete energy levels. Recently, several paradigms for spatial confinement of polaritons in semiconductor devices have been established [7–10]. This opens the way to quantum devices in which polaritons can be used as a vector of quantum information [11]. Their electronic component can be accessed and controlled optically, through their photonic component. This holds promise for preparation of quantum states, which might then be transferred to longer lived elements of quantum storage (e.g. localized spins), or as a mechanism for mediating interactions between such elements over long distances, as proposed in [12]. Precise control of the polariton wave function is then an essential requirement.

In this letter we demonstrate the manipulation of the wave function of confined zero dimensional (0D) exciton-polaritons under resonant optical excitation. The excited wave functions are monitored by collecting the coherent emission from the polariton traps. Control of the spatial and momentum probability distribution of the confined polaritons is achieved by tuning either the incidence angle or the energy of the excitation beam. Our results are supported by numerical simulations based on the coupled Gross-Pitaevskii equations for excitons and photons.

The sample we used to carry out our studies consists of a single quantum well embedded in a planar microcavity with a pattern of differently sized round mesas on the spacer layer [13]. Patterning the cavity thickness results in a modulation of the photon resonance energy, which corresponds to a potential trap, with finite energy barriers, able to confine polaritons. The confined polariton modes are then characterized by a discrete energy spectrum and spatially confined patterns [10, 14].

For our experiments we employed a photoluminescence setup in transmission configuration. The polaritons have been optically excited with a tunable cw Ti:Sa laser. The laser beam has been focused on the sample with a camera objective (f=55 mm and 1.2 aperture) providing an excitation spot of about 25 to 30 μm for all measurements. This provides a narrow distribution in k-space, which allows for a precise control of the excitation. By displacing the beam with a retroreflector parallel to the middle axis of the camera lens we changed the incidence angle θ and thus the in-plane momentum $\mathbf{k}_{\parallel} = (k_x, k_y)$ transferred to the polaritons ($k_{\parallel} \propto \sin(\theta)/\lambda_{\text{laser}}$). For non resonant excitation the laser has been tuned at the first reflectivity minimum of the DBR's around 784 nm. The excitation power, which was about 5 mW for non resonant excitation and about 7 μW for resonant excitation, was chosen in such a way that the system would always be in the linear regime. On the detection side we collected the light with a microscope objective an performed two dimensional (2D) k-space imaging and spatially resolved spectroscopy.

Figure 1(a) shows the spatially resolved photoluminescence spectrum of a 9 μm mesa at negative detuning, under non-resonant excitation. One can clearly distinguish the confined lower (1481.3-1484 meV) and upper (1485.5-1489.5 meV) polariton states in the mesa as well as the continuum states of the polaritons from the surrounding planar microcavity. This energy spectrum corresponds

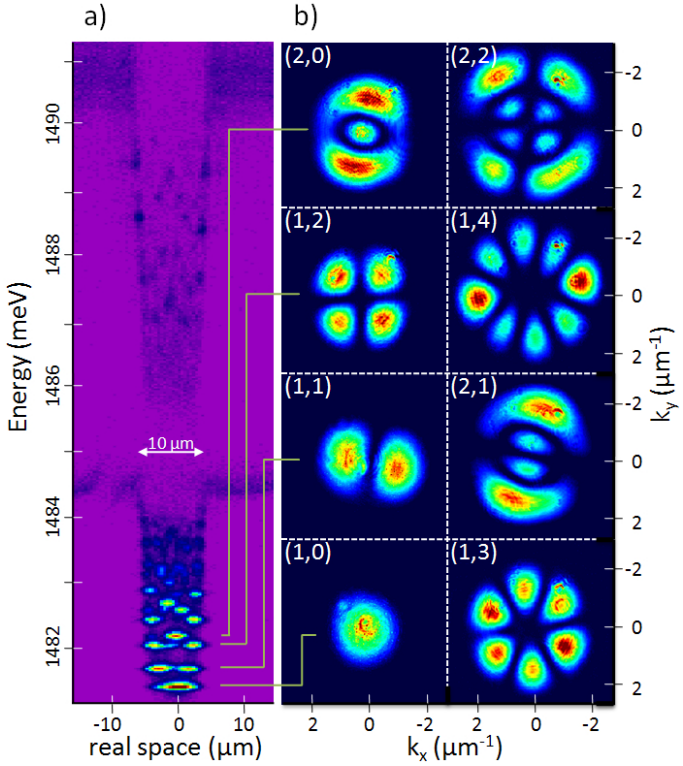

FIG. 1: (Color) (a) Real space spectrum of a 9 μm mesa at 2 meV negative detuning; upper and lower polariton branches of the 2D and 0D polaritons are clearly visible. (b) K-space images of resonantly excited states from the 0D lower polariton branch. The states can be labeled with two quantum numbers (n,m). $2\,|m|$ gives the number of nodes along ϕ on a full circle, while n corresponds to the number of lobes in radial direction.

well to what is expected from theory for a 9 μm trap with cylindrical symmetry [10, 14]. The eigenstates $|n, m\rangle$ can be labeled by a radial quantum number n $(1, 2, 3\ldots)$ and an angular quantum number m $(0, \pm1, \pm2\ldots)$ with no restriction over m [15]. The $\pm m$ states are degenerate due to the cylindrical symmetry of the potential.

Figure 1(b) shows the emission patterns in the 2D k-space of different confined lower polariton states. For this kind of measurements we excited the states resonantly in energy and $\mathbf{k}_\parallel$. In this case, the emission is dominated by the resonant linear response, while the photoluminescence due to energy relaxation is negligible [16]. The cylindrical symmetry of the trap should be visible in the observed emission pattern. However, Fig. (1(b) shows that the emission at the energies of the states with $|m| > 0$ and hence the polariton wave functions of these states feature lobes along the angular direction ϕ. These lobes are evidence of a breaking of the symmetry, which can come either from an anisotropy of the confinement potential or from the incidence angle of the excitation beam. In 9 μm mesas the anisotropy of the potential can be neglected in first approximation. The specific pattern comes from the coherent excitation of the $\pm m$ states at a $k_\parallel \neq 0$. The phases of the two eigenstates are locked at the laser position in k-space. Due to the angular dependence of the eigenstates wave functions ($\psi_{\pm m} \propto e^{\pm mi\phi}$), their phases evolve with opposite signs along ϕ. Since the observed image is proportional to $|\psi_{+m} + \psi_{-m}|^2$, the phase difference of the two components gives rise to positive and negative interferences along ϕ. The number of nodes on a full circle is hence equal to $2\,|m|$. The number of lobes in radial direction corresponds to n. The same conclusions hold for all degenerate m-doublets in all investigated mesas.

This phase locking effect can be used to manipulate the wave functions of degenerate doublet states. By changing the position of the excitation along ϕ in k-space, the phase of the $\pm m$ components is changed, and thus the interference pattern. This is demonstrated in Fig. 2 for the second excited state $(1, \pm2)$ in a 3 μm mesa. The intensity lobes follow the rotation of the laser. As the real space probability distribution shares the same symmetry as the momentum distribution, these results demonstrate also spatial control of the confined polariton wave functions. This offers a new degree of freedom for tuning the interaction between localised spins via polaritons, as proposed in [12].

Unlike the larger mesas, the 3 μm mesas have a non negligible ellipticity ($b/a \approx 1.29$), which can lift the degeneracy of $m = \pm1$ doublet states. This is the case

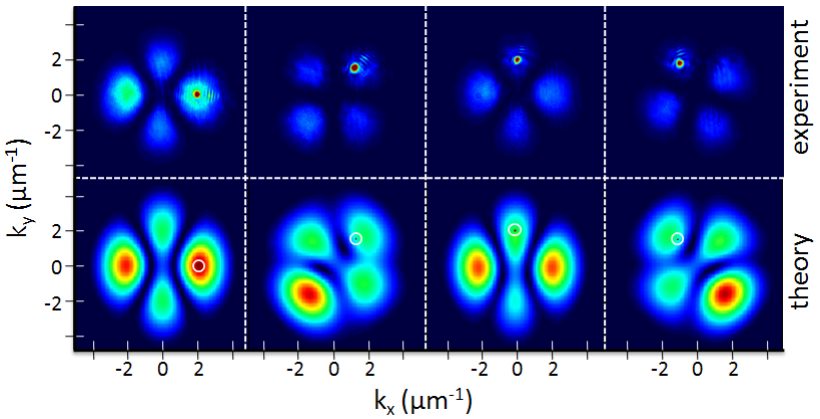

FIG. 2: (Color) Lobes of the degenerate second doublet state in a 3 μm mesa following the rotation of the laser in k-space. The mesa was at zero detuning. The upper part shows the experimental results and the theoretical results from the simulation are shown in the lower part of the figure. The red spot which is visible in each experimental image of this figure is an emission maximum arising from the laser light transmitted directly through the cavity beside the mesa. This makes it easy to observe the excitation angle. In the simulation images the laser position is marked by a circle.

for the first eigenstate doublet $|a\rangle$ and $|b\rangle$, which can be pictured as linear combinations of the $m = \pm 1$ states of a cylindrical structure with the same average diameter: $|a\rangle = \frac{1}{\sqrt{2}}(|1,-1\rangle + |1,+1\rangle)$ and $|b\rangle = \frac{1}{\sqrt{2}}(|1,-1\rangle - |1,+1\rangle)$. Therefore these eigenstates feature lobes along ϕ and their orientation is fixed by the axis of the ellipse. A degeneracy lift has only been observed for this lowest doublet state, as expected in theory. The splitting of the non-degenerate doublet increases with negative detuning due to the decreasing effective mass and is about 0.11 ± 0.04 meV at zero detuning. This agrees with the 0.08 meV expected from our model. If the splitting is large enough (> 0.1 meV) one can excite independently the $|a\rangle$ or $|b\rangle$ state at his eigenenergy. In this case the lobes do not follow the rotation of the laser since there is no longer interference between two eigenstates. The lobes will just vary in intensity depending on the overlap between the plane wave of the laser and the wave function of the eigenstate. At strong negative detuning the energy splitting becomes significantly larger than the natural linewidth of the modes (≈ 85 μeV) and since the laser spectral width is smaller (< 25 μeV), it is possible to excite only one state, but with different energies. Then the measured momentum pattern is that of the corresponding eigenstate.

Depending on the detuning, the momentum distribution of these split states can nevertheless be manipulated. In the case of a split doublet with sizeable spectral overlap, the laser energy can be tuned within the overlaping region between the eigenenergies of the two split states. As a consequence, it is then possible to vary the relative amplitude and phase of the two contributions to the linear response thanks to the different overlap of the laser with the two states. In this case one can rotate the polariton momentum distribution not only by rotating the laser momentum $\mathbf{k}_\parallel$ as shown before, but also by varying the laser energy. This offers additional control: by tuning the laser energy one can control the orientation of the lobes with respect to the laser position in k-space. Figure 3 shows the results of an experiment where we kept the excitation position in k-space constant and changed the excitation energy between two split states with significant spectral overlap.

As the figures 2 and 3 show, the experimental results presented here can be reproduced with a theoretical model which is described into more detail in [17]. We start from the bosonic exciton-photon Hamiltonian [18, 19] and we adopt a linearized mean-field approach [20]. In this approach and considering a coherent monochromatic optical pump $F(\mathbf{r},t) = e^{-i\omega t}F_0(\mathbf{r})$, the coherent exciton and photon fields $\Phi_{x,c}(\mathbf{r},t)$ evolve with the frequency of the laser source as $\Phi_{x,c}(\mathbf{r},t) = e^{-i\omega t}\Phi^0_{x,c}(\mathbf{r})$. Their steady-state shape $\Phi^0_{x,c}(\mathbf{r})$ obeys a set of two coupled Schrödinger-like equations for the exciton-photon problem [18, 20]

$$\left(-\frac{\hbar^2\nabla^2}{2m_x} - \hbar\omega - i\gamma_x\right)\Phi^0_x(\mathbf{r}) = \hbar\Omega_R\Phi^0_c(\mathbf{r})\,, \qquad (1)$$

$$\left(\epsilon_c(\vec{\nabla}) + U_c(\mathbf{r}) - \hbar\omega - i\gamma_c\right)\Phi^0_c(\mathbf{r}) = \hbar\Omega_R\Phi^0_x(\mathbf{r}) + F(\mathbf{r})\,, \qquad (2)$$

where m_x is the exciton mass, $\epsilon_c(k)$ is the cavity photon dispersion accounting for the photon-exciton detuning, U_c is the photon confining potential, $\hbar\Omega_R$ is the exciton-photon coupling and the decay rates $\gamma_{x,c}$ account for the finite lifetime of the two species. Here we are omitting the non-linear terms because we are interested in the linear regime (see discussion below). From these equations, it is clear that the phase of the coherent fields $\Phi_{x,c}(\mathbf{r},t)$ generated by the coherent pumping is locked to the phase

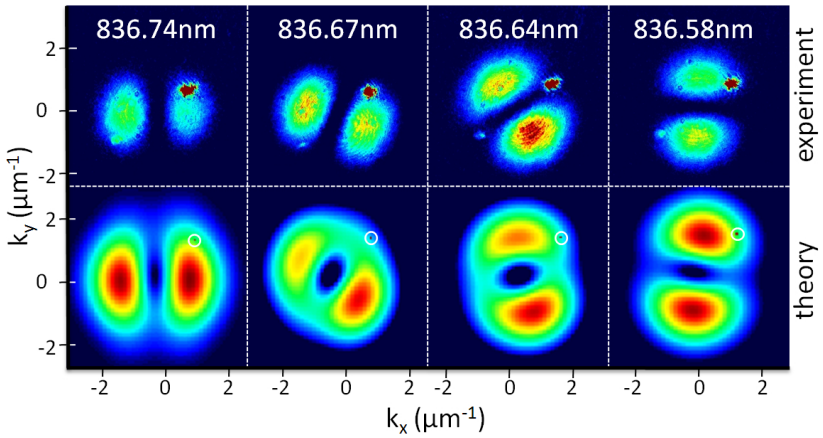

FIG. 3: (Color) Manipulation of the wave functions of the split first doublet in a 3 μm mesa ($\approx$ 3 meV negative detuning) by changing the excitation energy while keeping the excitation point constant. Upper part: experiment; Lower part: theoretical results. The polariton lifetime in our sample is about 15 ps, which leads to an energy linewidth of the eigenstates much broader than the spectral width of the laser. The lobes rotate due to the different contributions of the eigenstates to the linear response.

of the laser source. The coherent fields in k-space are obtained from the fields $\Phi^0_{x,c}(\mathbf{r})$ via Fourier transform.

From Eqs. (1) and (2), we see that the exciton coherent field is expected to have the same shape as the photon field, i.e. $\Phi^0_x(\mathbf{r}) \equiv X\Phi^0_p(\mathbf{r})$ and $\Phi^0_c(\mathbf{r}) \equiv C\Phi^0_p(\mathbf{r})$, as a result of the exciton-photon coupling. The relative intensity defines the exciton amount as

$$| X |^2 = \frac{\int d\mathbf{r} \mid \Phi^0_x(\mathbf{r}) \mid^2}{\int d\mathbf{r} \mid \Phi^0_p(\mathbf{r}) \mid^2}, \qquad (3)$$

where $|\Phi^0_p(\mathbf{r})|^2 = \mid \Phi^0_x(\mathbf{r}) \mid^2 + \mid \Phi^0_c(\mathbf{r}) \mid^2$. This clearly proves that, since $|X|^2 \sim 0.5$, the reported manipulation of the emitted optical field also implies the manipulation of the matter field.

For the calculations, we use a confining potential in agreement with AFM images of the mesas, thus accounting for the weak ellipticity of the samples. The decay rates are assumed to be $\gamma_c = 0.05$ meV, in agreement with the reported photon lifetime $\tau_c = 15$ ps, and $\gamma_x = 0.01$ meV. The other parameters are obtained from the experimental characterization of the sample [10, 13, 14].

The effect of polariton-polariton interactions could be very important, especially in presence of spatial confinement. By including the non-linear terms in Eqs. (1,2) [20] we have checked that this is not the case for the pump intensities used in this experiment. Therefore, all the reported features are entirely due to the linear response of the polariton system to resonant laser excitation.

In conclusion we have demonstrated different ways to manipulate the wave function of trapped zero-dimensional quasi-particles by optical means. The experimental results have been explained and reproduced in the frame of a theoretical model based on the Gross-Pitaevskii equations. Essential for the manipulation is a phase locking effect which locks the phase of the coherent polariton state to the phase of the laser at the excitation point in k-space. The spatial and the momentum probability distribution of the confined polariton wave function can thus be controlled by tuning the excitation conditions (incidence angle and energy). Therefore this phase locking effect could be used to manipulate the electromagnetic coupling of a mesa to a nearby system.

ACKNOWLEDGEMENTS

This work was supported by the Quantum Photonics NCCR and the Swiss National Science Foundation.

* E-mail: roland.cerna@epfl.ch
† Present address: CNR-INFM BEC Center and Dipartimento di Fisica, Universit di Trento, via Sommarive 14, I-38050 Povo, Trento, Italy
‡ Present address: Institut Néel-CNRS, 25 Avenue des Martyrs, BP 166, 38042 Grenoble Cedex 9, France
§ Present address: Institut des Nanotechnologies de Lyon (INL), UMR CNRS 5270, Ecole Centrale de Lyon, 36 Avenue Guy de Collongue, 69134 Ecully Cedex, France

[1] J. Kasprzak, M. Richard, S. Kundermann, A. Baas, P. Jeambrun, J. M. J. Keeling, F. M. Marchetti, M. H. Szymańska, R. André, J. L. Staehli, V. Savona, P. B. Littlewood, B. Deveaud & Le Si Dang, Nature (London) **443**, 409 (2006).
[2] H. Deng, G. S. Solomon, R. Hey, K. H. Ploog & Y. Yamamoto, Phys. Rev. Lett. **99**, 126403 (2007).
[3] R. M. Stevenson, V. N. Astratov, M. S. Skolnick, D. M. Whittaker, M. Emam-Ismail, A. I. Tartakovskii, P. G. Savvidis, J. J. Baumberg & J. S. Roberts, Phys. Rev. Lett. **85**, 3680 (2000).

[4] P. G. Savvidis, J. J. Baumberg, R. M. Stevenson, M. S. Skolnick, D. M. Whittaker & J. S. Roberts, Phys. Rev. Lett. **84**, 1547 (2000).
[5] M. Romanelli, C. Leyder, J. P. Karr, E. Giacobino & A. Bramati, Phys. Rev. Lett. **98**, 106401 (2007).
[6] S. Savasta, O. DiStefano, V. Savona & W. Langbein, Phys. Rev. Lett. **94**, 246401 (2005).
[7] D. Bajoni, E. Peter, P. Senellart, J. L. Smirr, I. Sagnes, A. Lematre & J. Bloch, Appl. Phys. Lett. **90**, 051107 (2007).
[8] R. Balili, V. Hartwell, D. Snoke, L. Pfeiffer & K. West, Science **316**, 1007 (2007).
[9] C. W. Lai, N. Y. Kim, S. Utsunomiya, G. Roumpos, H. Deng, M. D. Fraser, T. Byrnes, P. Recher, N. Kumada, T. Fujisawa & Y. Yamamoto, Nature (London) **450**, 529 (2007).
[10] R. I. Kaitouni, O. El Daif, A. Baas, M. Richard, T. Paraiso, P. Lugan, T. Guillet, F. Morier-Genoud, J. D. Ganière, J. L. Staehli, V. Savona, & B. Deveaud, Phys. Rev. B **74**, 155311 (2006).
[11] T. C. H. Liew, A. V. Kavokin & I. A. Shelykh, Phys. Rev. Lett. **101**, 016402 (2008).
[12] G. F. Quinteiro, J. Fernández-Rossier, & C. Piermarocchi, Phys. Rev. Lett. **97**, 097401 (2006).
[13] O. El Daif, A. Baas, T. Guillet, J. P. Brantut, R. I. Kaitouni, J. L. Staehli, F. Morier-Genoud, & B. Deveaud, Appl. Phys. Lett. **88**, 061105 (2006).
[14] A. Baas, O. El Daif, M. Richard, J. P. Brantut, G. Nardin, R. I. Kaitouni, T. Guillet, V. Savona, J. L. Staehli, F. Morier-Genoud, & B. Deveaud, Phys. Status Solidi B **243**, 2311 (2006).
[15] X. Leyronas & M. Combescot, Solid State Commun. **119**, 631–635 (2001).
[16] G. R. Hayes, S. Haacke, M. Kauer, R. P. Stanley, R. Houdré, U. Oesterle, & B. Deveaud, Phys. Rev. B **58**, R10175 (1998).
[17] D. Sarchi, M. Wouters & V. Savona, Phys. Rev. B **79**, 165315 (2009).
[18] D. Sarchi & V. Savona, Phys. Rev. B **77**, 045304 (2008).
[19] S. B. de-Leon & B. Laikhtman, Phys. Rev. B **63**, 125306 (2001).
[20] I. Carusotto & C. Ciuti, Phys. Rev. B **72**, 125335 (2005).
[21] G. Panzarini & L. C. Andreani, Phys. Rev. B **60**, 16799 (1999).